Biosensors and Bioelectronics 91 (2017) 804–810

Contents lists available at ScienceDirect

Biosensors and Bioelectronics

journal homepage: www.elsevier.com/locate/bios

Highly stable aluminum-based metal-organic frameworks as biosensing platforms for assessment of food safety

Chun-Sen Liu, Chun-Xiao Sun, Jia-Yue Tian, Zhuo-Wei Wang, Hong-Fei Ji, Ying-Pan Song, Shuai Zhang, Zhi-Hong Zhang*, Ling-Hao He, Miao Du*

Henan Provincial Key Laboratory of Surface & Interface Science, Zhengzhou University of Light Industry, Zhengzhou 450002, PR China

ARTICLE INFO

Keywords:
Al-MOFs
Crystal structures
Al-MOF-based electrochemical biosensors
Ultrasensitive detection

ABSTRACT

Two unique immunosensors made of aluminum-based metal-organic frameworks (MOFs), namely, 515- and 516-MOFs, with 4,4',4"-nitrilotribenzoic acid (H_3NTB) were successfully obtained to efficiently assess food safety. The as-prepared 515- and 516-MOFs exhibited superior thermal and physicochemical stability, high electrochemical activity, and good biocompatibility. Among these immunosensors, 516-MOF showed a preferable biosensing ability toward analytes determined by electrochemical techniques. The developed 516-MOF-based electrochemical biosensor not only demonstrated high sensitivity with low detection limits of 0.70 and 0.40 pg mL^{-1} toward vomitoxin and salbutamol, respectively, but also showed good selectivity in the presence of other interferences. Therefore, with the advantages of high sensitivity, good selectivity, and simple operation, this new strategy is believed to exhibit great potential for simple and convenient detection of poisonous and harmful residues in food.

1. Introduction

Considering the increasing rate of morbidity and mortality worldwide, foodborne illnesses have become a global concern (Cho et al., 2014; Pinu, 2016; Vaisocherová-Lísalová et al., 2016). Pollution components such as bacterial pathogens, illegal food additives, or heavy metal ions can come into contact with food products at any step in food preparation (Chavan et al., 2015; Chen et al., 2015; Connolly et al., 2011; Miller and Celli, 2016; Song et al., 2016; Yang et al., 2016). For instance, highly toxic secondary metabolites, such as vomitoxin (also known as deoxynivalenol), may widely exist in food products like maize, peanuts, milk products, and so on when they are stored improperly (Pinotti et al., 2016). Vomitoxin is one of the most widespread cereal contaminants worldwide. The US Food and Drug Administration has suggested an action level of 1 ppm for vomitoxin in foods intended for human consumption (Administration, 1994; Pestka, 2007). The main toxic effect of vomitoxin is the inhibition of protein and nucleic acid synthesis via ribosomal binding and by activating the cellular kinases involved in signal transduction, thereby resulting in decreased cell proliferation (Gu et al., 2015). The intake of vomitoxin can cause vomiting, abdominal pain, jaundice, edema, liver cancer, and even death. However, chemically stable vomitoxin cannot be completely resolved by traditional cooking conditions like oven or microwave heating. Moreover, vomitoxin presents an easy access to natural agricultural products when the temperature is approximately 30 °C or the crops are stored in a highly humid environment (Cardwell, 2000). Thus, highly sensitive, selective, and feasible methods are important for the detection of vomitoxin to ensure food security. In addition, salbutamol has been widely used as an additive in feeds of meat animals to change the metabolic pathways of nutrients. Salbutamol is a short β2-adrenergic receptor used to clinically treat bronchial asthma. Salbutamol can be accumulated in animal organs and can enter the human body through the food chain. High salbutamol content in the human body can cause nausea, aches, quivering hands, dizziness, and other symptoms of poisoning. Nevertheless, salbutamol is still widely used in animal feeds and illegally in many farms because it increases profits (Cui et al., 2012). Therefore, biosensors or immunosensors for salbutamol detection are particularly important.

Numerous methods were developed for the evolution of food safety; these strategies included atomic absorption spectrometry (Zhuravlev et al., 2015), atomic fluorescence spectrometry (Fernandez-Martinez et al., 2015), inductively coupled plasma–mass spectrometry (Ozcan et al., 2016), electrochemical biosensors (Amine et al., 2006), optical immunoassays (Vinayaka and Thakur, 2010), fluorescence arrays (Li et al., 2016a), immunochromatographic assays (Wu et al., 2016), and mass-sensitive immunosensors. Consequently, a simple, rapid, and accurate method for the detection of trace pollution components

* Corresponding authors.
E-mail addresses: mainzhh@163.com (Z.-H. Zhang), dumiao@public.tpt.tj.cn (M. Du).

http://dx.doi.org/10.1016/j.bios.2017.01.059
Received 24 November 2016; Received in revised form 18 January 2017; Accepted 25 January 2017
Available online 26 January 2017
0956-5663/

should be developed. Considering the advantages of high sensitivity and selectivity, low cost, miniaturization, and high compatibility with advanced micro-machining technologies, electrochemical biosensors have received much attention in the field of environmental monitoring and food quality control (Rotariu et al., 2016). Amounts of nanomaterials were coated with silica, zeolites, and carbon materials as electrode modifiers or carriers for the immobilization of biomolecules in electrochemical biosensors to improve their analytical performance (Zheng et al., 2009).

As well-defined porous crystalline materials, metal-organic frameworks (MOFs), which were constructed from metal centers/clusters and functional organic ligands, were explored as a new class of functional materials for applications in electrochemical fields, such as fuel cells (Xia et al., 2015), lithium-ion rechargeable batteries (Sunday et al., 2015), supercapacitors (Sun et al., 2015), solar cells (Hsu et al., 2014), and Li-S batteries (Li et al., 2016b). Compared with other conventional chemosensory materials, the definite and adjustable lattice structures of MOFs provided the most advantage in developing novel sensor devices. Accordingly, MOF-based biosensing techniques presented significant potential in fabricating powerful analytical sensors to detect analytes in clinical, environmental, and industrial applications (Kumar et al., 2015). However, applications of MOFs in biosensing and biomedical fields were limited by their low hydrolytic and stability (Guillerm et al., 2012). Therefore, the combination of MOF materials with other components and the special fabrication of biosensing avenues were undertaken to overcome the abovementioned limitations (Ling et al., 2016; Shen et al., 2016; Xie et al., 2015). In addition, compared with MOFs containing divalent d-block metals (especially Zn^{II} or Cu^{II}) and trivalent f-block lanthanides (He et al., 2014; Lu et al., 2014; Zhang and Cheng, 2015), trivalent Al(III) ion was shown to be a promising candidate for constructing various coordination frameworks with notable porosity, low density, and high thermal or physicochemical stability (Alvarez et al., 2015; Gaab et al., 2012).

However, no investigation on MOF applications in the determination of food safety has been reported. Therefore, researchers should directly develop new electrochemical immunosensors for determining poisonous and harmful residues in the environment. The present study introduced two bioactive Al-MOF-based immunosensors in which Al-MOF materials $\{[Al_3(\mu_3\text{-}O)(NTB)_2(H_2O)_3](NO_3)(NMF)_{10}(H_2O)_{7.5}\}_n$ (515-MOF) and $\{[Al_4(OH)_4(H_2O)(NTB)_2(HCOO)_3](HCOO)(NMF)_{14.5}(H_2O)_4\}_n$ (516-MOF) were synthesized by employing 4,4',4"-nitrilotribenzoic acid (H_3NTB) linker. To optimize Al-MOF-based immunosensors for the detection of trace analytes, the compared electrochemical biosensing systems were proposed for the detection of two antigens, including vomitoxin and salbutamol (Scheme 1). This work aims to provide a universal approach in designing desired electrochemical biosensors to specifically detect traces of targeted analytes with three advantages: (i) facile fabrication of electrochemical biosensors through direct usage of Al-MOFs with good basic comprehensive properties; (ii) high biosensing performances with high sensitivity, selectivity, and stability caused by the molecular recognition between the antibodies and antigen molecules; and (iii) broadening of the application of MOFs in food safety.

2. Experimental

2.1. Materials and methods

The ligand 4,4',4"-nitrilotribenzoic acid (H_3NTB) was prepared as described in the literature (Wang et al., 2011); other chemicals for 515- and 516-MOF materials were commercially available without further purification. Oxytetracycline (TET), doxycycline (DOX), kanamycin, ofloxacin, streptomycin (1.0 ng mL^{-1}), vomitoxin, salbutamol, the antibody of vomitoxin ($Anti_{vomitoxin}$), and the antibody of salbutamol($Anti_{salbutamol}$) were obtained from Solarbio Life Sciences Co., Ltd. Both $[Fe(CN)_6]^{-3/-4}$ and phosphate-buffered solution (PBS) (pH 7.4, NaCl; Na_2HPO_3; KH_2PO_4; KCl) were obtained from Aladdin Co., Ltd. All other chemicals used in this study were analytical grade reagents.

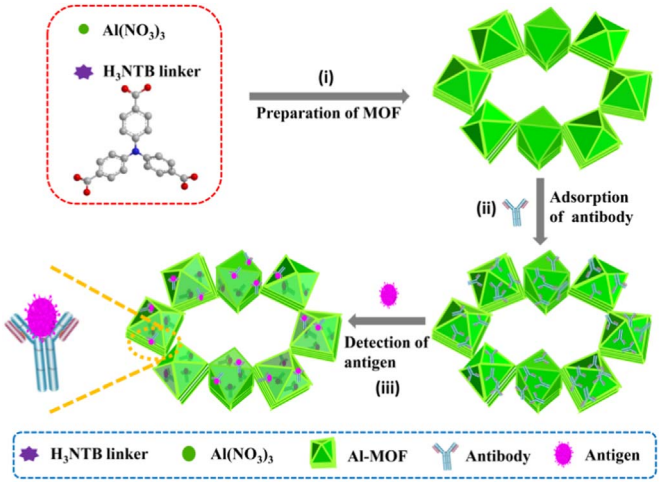

Scheme 1. Schematic of the fabrication of electrochemical biosensing based on Al-MOFs (515- and 516-MOFs) for detection of antigen: (i) preparation of Al-MOFs, (ii) adsorption of antibody, and (iii) detection of antigen.

2.2. Fabrication of the electrochemical immunosensors based on 515- and 516-MOFs

To develop the immunosensors, 515- and 516-MOFs were dispersed into fresh Milli-Q water at concentration of 1.0 mg mL^{-1}. The prepared solutions (10.0 μL) were dropped into clean gold electrodes. Finally, the modified electrodes were dried in N_2 stream for further testing. The modified AEs were incubated separately with the solutions of $Anti_{vomitoxin}$ and $Anti_{salbutamol}$ for 2 h (Anti/Al-MOFs/AE) at room temperature. Subsequently, the modified AEs adsorbed with antibodies were sufficiently rinsed with PBS and then dried over a gentle stream of nitrogen, through which the developed immunosensors were accomplished. Further measurements were performed. When not in use, the immunosensors were stored at 4 °C in a refrigerator.

2.3. Electrochemical measurements

All electrochemical measurements, including Electrochemical impedance spectroscopy (EIS) and cyclic voltammetry (CV), were conducted on a CHI660D electrochemical workstation (Shanghai Chenhua, China). A conventional three-electrode system, which included a gold electrode with a diameter of 3 mm as a working electrode, an Ag/AgCl (saturated KCl) electrode as a reference electrode, and a platinum slide as a counter electrode, was used. EIS curves were obtained in 0.5 mM $[Fe(CN)_6]^{3-/4-}$ containing 0.1 M KCl (EIS parameters: potential, 0.21 V; frequency range, 100–0.1 Hz; amplitude, 5 mV; room temperature). Incubation and test temperature are room-temperature. The EIS spectra were analyzed using Zview2 software, which utilizes nonlinear least-squares fitting to determine element parameters in the equivalent circuit.

3. Results and discussion

3.1. Chemical structures and components of pure Al-MOFs and their films

XPS measurement was performed to investigate the chemical components of the pure Al-MOFs powders and the related films coated onto the silicon wafers. In the XPS survey scan spectra of 516- and 516-MOFs (Fig. S9), substantial C 1*s* and O 1*s* signals were observed, whereas signals of N 1*s* and Al 2*p* appeared to be very weak. In the case

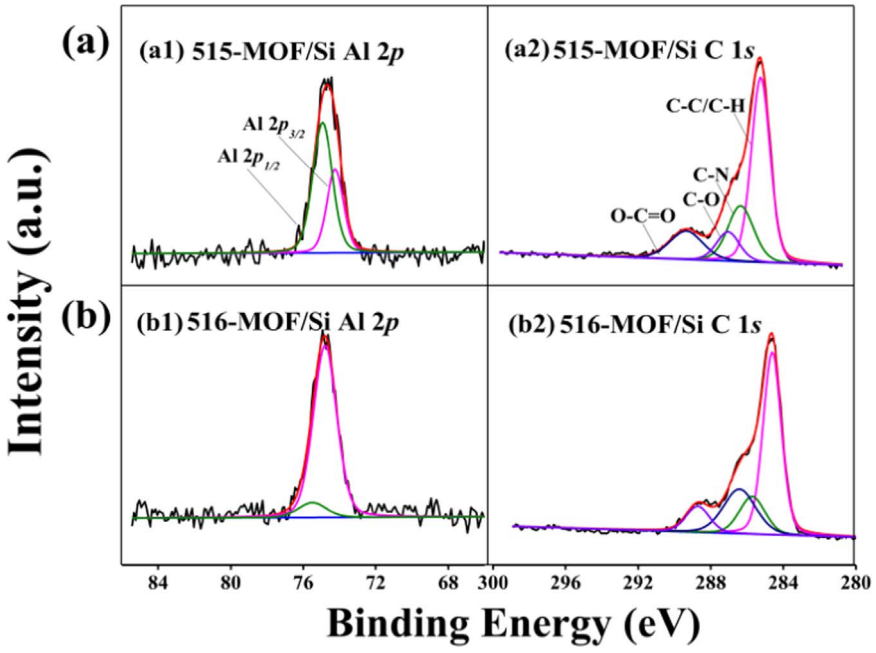

Fig. 1. High-resolution Al 2*p* and C 1*s* XPS spectra of (a) 515- and (b) 516-MOF films on silicon wafers.

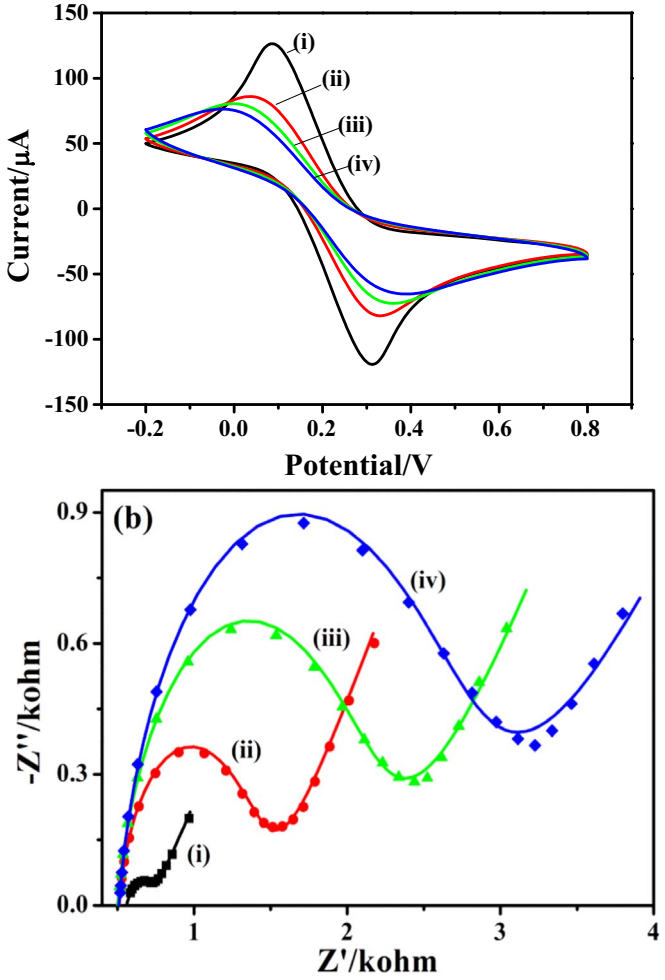

Fig. 2. (a) CV at a scan rate of 100 mVs^{-1} and (b) Nyquist of EIS (i) the gold electrode, (ii) MOFs, (iii) $Anti_{vomitoxin}$, and (iv) 0.001 ng mL^{-1} vomitoxin. Both measurements were recorded in 5 mM $Fe(CN)_6^{3-/4-}$ (0.1 M PBS pH 7.4) contained in 0.14 M NaCl and 1 M KCl of 516 MOF@$Anti_{vomitoxin}$-based electrochemical biosensor for detection of vomitoxin.

of the Al-MOF-related films, in which the Al-MOF powders were dispersed into water and spin-coated in the silicon wafer, an additional signal of Si 2*p* was obtained because of the presence of the substrate. Moreover, the relative intensity of each element was changed because of the possible interaction between Al-MOFs and water molecules. Therefore, the atom% of each element, including C 1*s*, O 1*s*, N 1*s*, and Al 2*p*, was collected, and the results are summarized in Table S4. In comparison with the Al-MOF powders, the atom% of C 1*s* and Al 2*p* of the corresponding films decreased, whereas the atom% of O 1*s* increased. This result can be explained by the replacement of the Al–O–C coordination by the Al–O–H because of the addition of H_2O molecules (Yu et al., 2015a, 2015b).

To understand the chemical environment of each element contained in the samples, the high-resolution XPS spectra of Al 2*p* and C 1*s* were decomposed. The Al 2*p* core-level binding energy (Fig. S10a1 and b1) was deconvoluted in two distinct components at 74.7 and 75.4 eV, which were attributed to Al $2p_{3/2}$ and Al $2p_{1/2}$ (Yu et al., 2015a, 2015b). When coated in the silicon wafers (Fig. 1a1 and b1), the peaks of Al $2p_{3/2}$ and Al $2p_{1/2}$ were shifted to 75.0 and 75.7 eV because of the variation of chemical environments around the Al atoms (Kim and Manthiram, 2015). Moreover, the high-resolution XPS spectra of C 1*s* of the powder samples can be fitted into four parts, namely, 284.6, 285.7, 288.7, and 291.7 eV, which were assigned to the groups of C–C/C–H, C–N, COO–, and C–F_2, respectively. The first three peaks originated from the organic ligands contained in the framework of the MOF materials. The C–F_2 group was attributed to the reservation of the trifluoroacetic acid used to prepare the Al-MOFs. However, for the film samples, an additional peak at 286.4 eV, C–O, resulted because the difference in the coordination types between Al and O atoms changed. The peak at 291.7 eV of C–F_2 was not attained because of the release of trifluoroacetic acid into the water medium.

3.2. Comparison of the electrochemical biosensing performances of 515- and 516-MOF-based immunosensors

CVs and EIS measurements were performed to evaluate each stage of the electrochemical immunosensor in detecting vomitoxin and salbutamol. The typical CV curves of different modified electrodes in 1.0 mM $[Fe(CN)_6]^{3-/4-}$ mixture solution containing 0.1 M KCl is shown in Fig. 2a. A pair of clear redox peaks was observed for the

bare AE (curve i, Fig. 2a), corresponding to the electron transfer of the $[Fe(CN)_6]^{3-/4-}$ couple. For 516-MOF/AE (curve ii, Fig. 2a), the redox peaks of $[Fe(CN)_6]^{3-/4-}$ decreased evidently with the increase in peak-to-peak separation, indicating that the electron transfer of $[Fe(CN)_6]^{3-/4-}$ at the electrode surface was hindered by the coverage of 516-MOF. This result can be explained by the relative poor electrochemical performances ascribed to the presence of the organic phase contained in 516-MOF (Hsu et al., 2014). Subsequently, the decrease in the redox peaks of $[Fe(CN)_6]^{3-/4-}$ was obtained after the composite electrode was incubated with the $Anti_{vomitoxin}$ solution for 2 h (curve iii, Fig. 2a), suggesting the strong adsorption of $Anti_{vomitoxin}$ on the modified electrode. After addition of 1.0 pg mL^{-1} vomitoxin, the redox peaks of $[Fe(CN)_6]^{3-/4-}$ on the developed immunosensor decreased (curve iv, Fig. 2a). The results suggested that vomitoxin was successfully captured by $Anti_{vomitoxin}$/516-MOF/AE through the immunoreaction between antibody and antigen (Yang and Li, 2005). As a result, the thickening of the non-conductive sensing layer hindered the electron transfer of $[Fe(CN)_6]^{3-/4-}$. This determination behavior illustrated that the prepared sensor of $Anti_{vomitoxin}$/516-MOF/AE was feasible for the determination of vomitoxin.

EIS measurement was performed to investigate the surface features of the modified electrode at each immobilization step (Li et al., 2014; Sezginturk, 2011). The Nyquist plots of AC impedance spectroscopy were recorded from 0.1 Hz to 10^5 Hz at 0.21 V in a solution containing 0.1 M KCl and 2.5 mM $[Fe(CN)_6]^{3-/4-}$. Fig. 3b shows the EIS Nyquist plots observed during the stepwise modification processes. The typical impedance spectroscopy was composed of a semicircle portion at higher frequencies representing the charge-transfer resistance (R_{ct}) and a linear part at lower frequencies corresponding to the diffusion process. The R_{ct} value was deduced from the semicircle diameter of EIS Nyquist plots at high frequency range (Gaab et al., 2012; Kang et al., 2009; Patolsky et al., 1999), which represented the charge-transfer kinetics of the $[Fe(CN)_6]^{3-/4-}$ redox system (Fig. S13). Also, the equivalent circuit used in the simulation the Nyquist curves was supplied in the inset of Fig. S13. AE exhibited a small resistance, suggesting that it behaved as a good electron conductor with low resistance. The R_{ct} value of AE was 30 Ω (curve i, Fig. 2b). After modification with 516-MOF, the R_{ct} value of the composite electrode (curve ii, Fig. 2b) was 0.75 kohm. The R_{ct} value significantly increased, which was attributed to the reduced electrochemical activity of Al-MOFs and led to the decrease in the electron transfer (Kaur et al., 2016). However, when $Anti_{vomitoxin}$ was adsorbed onto the 516-MOF/AE (curve iii, Fig. 2b), the R_{ct} value was increased to 1.37 kohm. The results indicated that $Anti_{vomitoxin}$ was successfully immobilized in the composite electrode, and the protein film blocked the electron transfer between the base solution and electrode (Du et al., 2008). After detection of vomitoxin, the R_{ct} value of vomitoxin/$Anti_{vomitoxin}$/516-MOF/AE (curve iv, Fig. 2b) was 1.80 k ohm. The gradually increased impedance of the composite electrode surface demonstrated that the highly specific immune recognition hindered the electronic conductivity (Loaiza et al., 2011). Overall, the results suggested that the 516-MOF-based electrochemical immunosensors were fabricated to present an excellent recognition ability toward target molecules.

To compare the determination performance of the 516-MOF-based biosensing system, another kind of Al-MOF, 515-MOF, was employed as a platform of the electrochemical immunosensors in detecting vomitoxin. However, given the poor water stability of 515-MOF, it was difficult to be tightly coated on the electrode surface. Nevertheless, similar electrochemical measurements in vomitoxin determination were performed using the 515-MOF-based electrochemical immunosensor (Fig. S14). The obtained results and detection behavior of vomitoxin were similar to those of the 516-MOF-based biosensing system. The 515-MOF based immunosensor also exhibited highly sensitive variations in the electrochemical signals, as well as good detection efficiency of vomitoxin. Considering the usage requirement of the good reproducibility and stability of the electrochemical immunosensors, 516-MOF was selected for further electrochemical measurements.

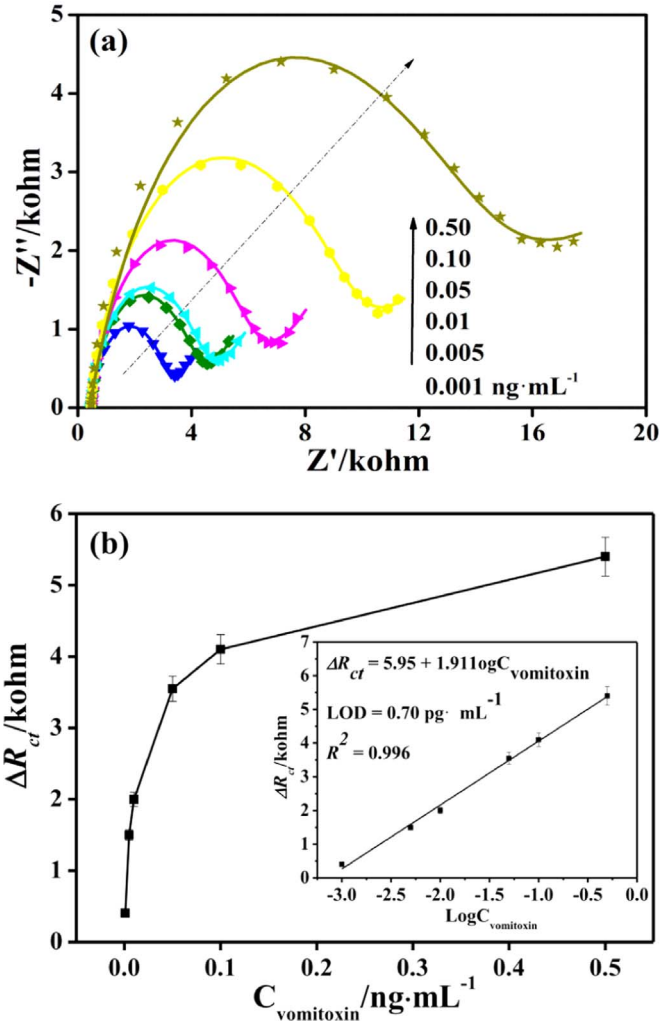

Fig. 3. (a) EIS response of $Anti_{vomitoxin}$/516-MOF/AE with different concentrations of vomitoxin (0, 0.001, 0.005, 0.01, 0.05, 0.1, and 0.5 ng mL^{-1}); (b) dependence of ΔR_{ct} of the modified electrode on concentration of vomitoxin. The linear part of the calibration curve is shown in the inset of (b).

To forecast the generality of the novel developed strategy, the 516-MOF-based detection system was used to reveal harmful molecules in food products, specifically salbutamol. As shown in Fig. S13, a similar trend was observed for salbutamol detection using the fabricated immunosensors based on 516-MOF. As shown in the CV data (Fig. S15a), a continuous decrease was observed in the peak current with the detection procedure conducted. The adsorption of the $Anti_{salbutamol}$ and the bio-binding between the antibody and salbutamol showed an increase in the corresponding Rct values of each step (Fig. S15b). The data also illustrated that the antibody adsorption and the salbutamol detection hindered the electron transfer between the electrode surface and the electrolyte solution. The aforementioned condition led to the decrease in the CV diagrams and increase in the R_{ct} values of EIS plots. All of these results suggested that the developed electrochemical immunosensor based on 516-MOF can be used to monitor the fields of environmental protection and serve as a potential strategy to determine food safety.

3.3. Analytical performance

To evaluate the analytical performance of the developed immunosensors, the $Anti_{vomitoxin}$/Al-MOF/AE electrode was incubated with

different concentrations of vomitoxin and then electrochemically measured in $Fe[(CN)_6]^{3-/4-}$ solution through EIS. Fig. 3a shows the Nyquist plots of $Anti_{vomitoxin}$/Al-MOFs/AE upon immunoreaction with different concentrations of vomitoxin. The R_{ct} values gradually increased with the vomitoxin concentrations from 0.001 ng mL^{-1} to 0.5 ng mL^{-1} (Fig. 3b). The result was attributed to more antigen–antibody complexes formed on the electrode surface with the increasing vomitoxin concentrations, as well as the enhanced resistance of electron transfer of $Fe[(CN)_6]^{3-/4-}$ on the electrode surface. When the R_{ct}variation (ΔR_{ct}) of the immunosensor, before and after immunoreaction, was used as the sensing signal, the ΔR_{ct} value was proportional to the logarithm value of the vomitoxin concentration from 0.001 ng mL^{-1} to 0.5 ng mL^{-1}. The linear regression equation was ΔR_{ct}=1.906 log $C_{vomitoxin}$+5.95, with the correlation coefficient (R^2) of 0.996 (Fig. 3b). The detection limit (LOD) was estimated to be as low as 0.7 pg mL^{-1} at a signal-to-noise (S/N) ratio of 3.

To obtain the sensitivity of the salbutamol detection, the same determination approach was employed using the developed 516-MOF-based immunosensor (Fig. S16). The linear regression equation, ΔR_{ct}=0.781ogC$_{salbutamol}$ +2.66, was simulated. The LOD was estimated to be as low as 0.4 pg mL^{-1} at S/N ratio of 3 with the correlation coefficient (R^2) of 0.996 (Fig. S16b). Clearly, the analytical performances of the developed biosensors based on 516-MOF in detecting vomitoxin and salbutamol were superior to those of other reported biosensors (Table 1 and Table S5).

3.4. Selectivity, reproducibility, and stability of the developed immunosensors

To investigate the selectivity of the fabricated immunosensors, various interfering agents, including TET, DOX, kanamycin, ofloxacin, and streptomycin (0.10 ng mL^{-1}), were measured. The R_{ct} responses to each type of antigen are shown in Fig. 4a; even at 100-fold higher concentrations than that of vomitoxin (1.0 pg mL^{-1}), no evident change in the R_{ct} response was observed from the non-targets in contrast to the blank test. Nevertheless, a significant increase was found in the presence of vomitoxin. Moreover, the cross sensitivity of the biosensor in a mixture of five different substances containing vomitoxin was also examined (Fig. 4b). The obtained response from the mixture was almost the same as the response obtained from the individual vomitoxin only. The results validated the high selectivity of the proposed immunosensor.

The selectivity of the proposed immunosensor was probed by comparing the ΔR_{ct} values toward the solutions containing either salbutamol or other environmentally relevant constituents, such as RAC, CLB, K^+, Na^+, Urea, Ca^{2+}, and UA (0.10 pg mL^{-1} each). As shown in Fig. S17, the developed immunosensor exhibited substantial signal to the solution containing salbutamol (1.0 pg mL^{-1}), whereas a negligible signal was obtained from the solutions containing these interference components even at a 1000-fold higher concentration than that of salbutamol. This result indicated that the electrochemical immunosensor to salbutamol was hardly affected by the presence of an interfering constituent. The results suggested that the fabricated 516-MOF-based immunosensor exhibited high selectivity toward its target analytes. The precision of the developed immunosensor was parallel examined by detecting vomitoxin (1.0 pg mL^{-1}) and salbutamol (1.0 pg mL^{-1}) with the five modified electrodes bonded with the

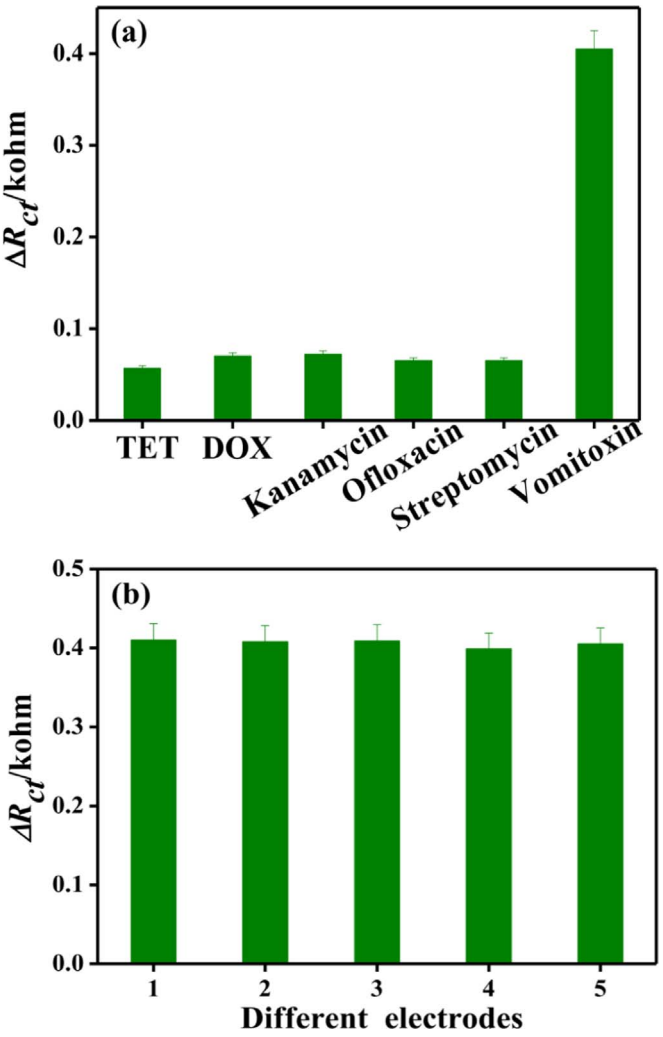

Fig. 4. Selectivity (a) and stability (b) studies of the 516-MOF-based electrochemical immunosensor toward vomitoxin. EIS experiments were performed with 1 ng mL^{-1} each of TET, DOX, kanamycin, ofloxacin, and streptomycin, as well as 0.001 ng mL^{-1} vomitoxin.

Table 1
Comparisons of the proposed method with other vomitoxin-detection methods.

Materials	Detection method	Line range	LOD	References
deoxynivalenol-3-glucoside	liquid chromatography/linear ion trap mass spectrometry method	10.0–200.0 μg kg^{-1}	30.0 μg kg^{-1}	(Suman et al., 2013)
anti- deoxynivalenol	differential pulse voltammetry (DPV)	0.01–1000.0 ng mL^{-1}	5.0 pg mL^{-1}	(Qing et al., 2016)
tris(bipyridine) ruthenium (II) chloride	EIS	6.0–30.0 ng mL^{-1}	0.3 μg mL^{-1}	(Sunday et al., 2015)
deoxynivalenol metabolism	Ultra performance liquid chromatography and Mass spectrometry	50–5000 ng·mL^{-1}	25.0 ng mL^{-1}	(Ran et al., 2013)
Quenchbody	liquid chromatography and Mass spectrometry	0.0003–3.0 mg mL^{-1}	0.006 mg mL^{-1}	(Yoshinari et al., 2015)
horse radish peroxidase as the label	Real-time electrochemical profiling	6.25–250.0 ng mL^{-1}	6.25 ng mL^{-1}	(Olcer et al., 2014)
516-MOF/$Anti_{vomitoxin}$	EIS	0.001–0.5 ng mL^{-1}	0.7 pg mL^{-1}	**This work**

antibodies of vomitoxin and salbutamol. The results showed that the relative standard deviation (RSD) for five determination systems of vomitoxin (Fig. 4b) and salbutamol (Fig. S17b) were 4.44% and 3.78%. Moreover, in each monitored system of vomitoxin and salbutamol, the same developed immunosensor was measured continuously for 15 days. Approximately 4.20% decrease in the *Rct* change in the detection of vomitoxin and 5.20% decrease in the R_{ct} change in the detection of salbutamol were noted after covering the samples with a glass beaker for 15 days at 4 °C in the refrigerator and then at room temperature; this finding indicated long-term storage and operational stability. Moreover, the developed immunosensor for detecting vomitoxin and salbutamol can be regenerated by rinsing the sensor surface using 0.1 M hydrochloric acid and 1% sodium dodecyl sulphate solution for 3 min, separately. The results illustrated that the fabricated immunosensor based on 516-MOF can be reused for ten times at least (Fig. S18). Overall, the results suggest that the fabricated determination sensor showed good precision, acceptable construction reproducibility, stability and regeneration.

3.5. Measurements on real samples

To explore the practical applications of the fabricated electrochemical immunosensor based on 516-MOF, it was employed to determine vomitoxin and salbutamol in wine and pork samples, respectively. Fifty-microliter aliquots of the supernatant of each sample were diluted with PBS for the determination procedure. For the recovery determination of vomitoxin, rice samples were spiked with different amounts of vomitoxin. The spiked samples with vomitoxin concentrations of 1.0 pg mL^{-1} were analyzed with five repetitive measurements each, and acceptable recoveries of 98.0–100.4% for vomitoxin were obtained (Table S6). For the applicability of the as-developed sensor in salbutamol detection, the pork samples were spiked with different amounts of salbutamol, and the recoveries of 99.6–101.6% were obtained (Table S7). These results suggested that the as-proposed electrochemical immunosensing system exhibited good anti-interference capability even in a complex system and is therefore effective in practical applications.

4. Conclusions

In summary, we proposed a simple, rapid, and highly sensitive electrochemical strategy in detecting vomitoxin and salbutamol This method is based on the unique Al-MOFs (515- and 516-MOFs) with high specific surface area and thermal or physicochemical stability, especially in water. This immunosensing system exhibits the advantages of good selectivity and high sensitivity of 0.7 and 0.4 pg mL^{-1} toward vomitoxin and salbutamol, respectively, and these values are superior to those reported in the literature. The merits lie in the fact that the high water stability, multi-functionality, high specific surface area, and relatively high electrochemical activity of Al-MOFs and the bio-recognition between antibody and antigen increases the convenience and efficiency of the assay. Thus, this developed strategy supplies a potential application of Al-MOFs in the field of environmental protection and food safety.

Acknowledgements

We are grateful to the support from the National Natural Science Foundation of China (21471134 and 21571158), Innovation Scientists and Technicians Troop Construction Projects of Henan Province (152101510003), Plan for Scientific Innovation Talent of Henan Province (154200510011), and Program for Science & Technology Innovative Research Team in University of Henan Province (15IRTSTHN-002).

Appendix A. Supplementary information

Supplementary data associated with this article can be found in the online version at doi:10.1016/j.bios.2017.01.059.

References

Administration, Food and Drug, 1994. (a) FDA (Food and Drug Administration) regulatory guidance for toxins and contaminants, 1994.
Alvarez, E., Guillou, N., Martineau, C., Bueken, B., Van de Voorde, B., Le Guillouzer, C., Fabry, P., Nouar, F., Taulelle, F., de Vos, D., Chang, J.S., Cho, K.H., Ramsahye, N., Devic, T., Daturi, M., Maurin, G., Serre, C., 2015. Angew. Chem. Int. Ed. 54 (12), 3664–3668.
Amine, A., Mohammadi, H., Bourais, I., Palleschi, G., 2006. Biosens. Bioelectron. 21 (8), 1405–1423.
Cardwell, K.F., 2000. Food Nutr. Bull. 21 (4), 488–492.
Chavan, A.A., Li, H., Scarpellini, A., Marras, S., Manna, L., Athanassiou, A., Fragouli, D., 2015. ACS Appl. Mater. Interfaces 7, 14778–14784.
Chen, H., Wang, X., Li, J., Wang, X., 2015. J. Mater. Chem. A 3 (11), 6073–6081.
Cho, I.-H., Mauer, L., Irudayaraj, J., 2014. Biosens. Bioelectron. 57, 143–148.
Connolly, L., Ropstad, E., Verhaegen, S., 2011. TrAC Trends Anal. Chem. 30 (2), 227–238.
Cui, Z.T., Cai, Y.Y., Wu, D., Yu, H.Q., Li, Y., Mao, K.X., Wang, H., Fan, H.X., Wei, Q., Du, B., 2012. Electrochim. Acta 69, 79–85.
Du, Y., Li, B.L., Wei, H., Wang, Y.L., Wang, E.K., 2008. Anal. Chem. 80 (13), 5110–5117.
Fernandez-Martinez, R., Rucandio, I., Gomez-Pinilla, I., Borlaf, F., Garcia, F., Larrea, M.T., 2015. J. Food Compos. Anal. 38, 7–12.
Gaab, M., Trukhan, N., Maurer, S., Gummaraju, R., Muller, U., 2012. Micropor. Mesopor. 157, 131–136.
Gu, W.S., Zhu, P., Jiang, D.L., He, X.X., Li, Y., Ji, J., Zhang, L.J., Sun, Y.G., Sun, X.L., 2015. Biosens. Bioelectron. 70, 447–454.
Guillerm, V., Ragon, F., Dan-Hardi, M., Devic, T., Vishnuvarthan, M., Campo, B., Vimont, A., Clet, G., Yang, Q., Maurin, G., Ferey, G., Vittadini, A., Gross, S., Serre, C., 2012. Angew. Chem. Int. Ed. 51 (37), 9267–9271.
He, Y.B., Li, B., O'Keeffe, M., Chen, B.L., 2014. Chem. Soc. Rev. 43 (16), 5618–5656.
Hsu, S.H., Li, C.T., Chien, H.T., Salunkhe, R.R., Suzuki, N., Yamauchi, Y., Ho, K.C., Wu, K.C.W., 2014. Sci. Rep., 4.
Kang, X.H., Wang, J., Wu, H., Aksay, I.A., Liu, J., Lin, Y.H., 2009. Biosens. Bioelectron. 25 (4), 901–905.
Kaur, R., Kim, K.H., Paul, A.K., Deep, A., 2016. J. Mater. Chem. A 4 (11), 3991–4002.
Kim, S.O., Manthiram, A., 2015. J. Mater. Chem. A 3 (5), 2399–2406.
Kumar, P., Deep, A., Kim, K.H., 2015. Trac-Trend Anal. Chem. 73, 39–53.
Li, C.L., Wen, K., Mi, T.J., Zhang, X.Y., Zhang, H.Y., Zhang, S.X., Shen, J.Z., Wang, Z.H., 2016a. Biosens. Bioelectron. 79, 258–265.
Li, X., Sun, Q., Liu, J., Xiao, B.W., Li, R.Y., Sun, X.L., 2016b. J. Power Sources 302, 174–179.
Li, Y.X., Afrasiabi, R., Fathi, F., Wang, N., Xiang, C.L., Love, R., She, Z., Kraatz, H.B., 2014. Biosens. Bioelectron. 58, 193–199.
Ling, P.H., Lei, J.P., Jia, L., Ju, H.X., 2016. Chem. Commun. 52 (6), 1226–1229.
Loaiza, O.A., Lamas-Ardisana, P.J., Jubete, E., Ochoteco, E., Loinaz, I., Cabanero, G., Garcia, I., Penades, S., 2011. Anal. Chem. 83 (8), 2987–2995.
Lu, W.G., Wei, Z.W., Gu, Z.Y., Liu, T.F., Park, J., Park, J., Tian, J., Zhang, M.W., Zhang, Q., Gentle, T., Bosch, M., Zhou, H.C., 2014. Chem. Soc. Rev. 43 (16), 5561–5593.
Miller, C., Celli, J., 2016. J. Mol. Biol. 428 (17), 3387–3398.
Olcer, Z., Esen, E., Muhammad, T., Ersoy, A., Budak, S., Uludag, Y., 2014. Biosens. Bioelectron. 62, 163–169.
Özcan, Ş., Bakirdere, S., Ataman, O.Y., 2016. Anal. Lett. 49 (15), 2501–2512.
Patolsky, F., Zayats, M., Katz, E., Willner, I., 1999. Anal. Chem. 71 (15), 3171–3180.
Pestka, J.J., 2007. Anim. Feed Sci. Tech. 137 (3–4), 283–298.
Pinotti, L., Ottoboni, M., Giromini, C., Dell'Orto, V., Cheli, F., 2016. Toxins 8 (2).
Pinu, F.R., 2016. Trends Food Sci. Tech. 54, 213–215.
Qing, Y., Li, C., Yang, X., Zhou, X., Xue, J., Luo, M., Xu, X., Chen, S., Qiu, J., 2016. J. Appl. Electrochem. 46 (10), 1049–1057.
Ran, R., Zhang, W., Cui, B., Xu, Y., Han, Z., Wu, A., Li, D., Zhang, D., Wang, C., Shi, J., 2013. Anal. Methods 5 (20), 5637–5643.
Rotariu, L., Lagarde, F., Jaffrezic-Renault, N., Bala, C., 2016. Trac-Trends Anal. Chem. 79, 80–87.
Sezginturk, M.K., 2011. Biosens. Bioelectron. 26 (10), 4032–4039.
Shen, W.J., Zhuo, Y., Chai, Y.Q., Yuan, R., 2016. Biosens. Bioelectron. 83, 287–292.
Song, C., Liu, J., Li, J., Liu, Q., 2016. Biosens. Bioelectron. 85, 734–739.
Suman, M., Bergamini, E., Catellani, D., Manzitti, A., 2013. Food Chem. 136 (3), 1568–1576.
Sun, Z.X., Xin, F.X., Cao, C., Zhao, C.C., Shen, C., Han, W.Q., 2015. Nanoscale 7 (48), 20426–20434.
Sunday, C., Masikini, M., Wilson, L., Rassie, C., Waryo, T., Baker, P., Iwuoha, E.I., 2015. Sensors 15 (2), 3854–3871.
Vaisocherová-Lísalová, H., Víšová, I., Ermini, M.L., Špringer, T., Song, X.C., Mrázek, J., Lamačová, J., Lynn, N.S., Šedivák, P., Homola, J., 2016. Biosens. Bioelectron. 80, 84–90.
Vinayaka, A.C., Thakur, M.S., 2010. Anal. Bioanal. Chem. 397 (4), 1445–1455.
Wang, J., He, C., Wu, P.Y., Wang, J., Duan, C.Y., 2011. J. Am. Chem. Soc. 133 (32), 12402–12405.
Wu, X.L., Huang, M.H., Yu, S.J., Kong, F.S., 2016. Food Chem. 190, 843–847.
Xia, W., Mahmood, A., Zou, R.Q., Xu, Q., 2015. Energy Environ. Sci. 8 (7), 1837–1866.

Xie, S.B., Ye, J.W., Yuan, Y.L., Chai, Y.Q., Yuan, R., 2015. Nanoscale 7 (43), 18232–18238.
Yang, L.J., Li, Y.B., 2005. Biosens. Bioelectron. 20 (7), 1407–1416.
Yang, T., Huang, H., Zhu, F., Lin, Q., Zhang, L., Liu, J., 2016. Sensors 16 (7), 1118.
Yoshinari, T., Ohashi, H., Abe, R., Kaigome, R., Ohkawa, H., Sugitakonishi, Y., 2015. Anal. Chim. Acta 888, 126–130.
Yu, Q., Meng, X.G., Wang, T., Li, P., Ye, J.H., 2015a. Adv. Funct. Mater. 25 (18), 2686–2692.
Yu, Y.H., Li, Z.D., Wang, Y.M., Gong, S.Q., Wang, X.D., 2015b. Adv. Mater. 27 (33), 4938–4944.
Zhang, S.W., Cheng, P., 2015. CrystEngComm 17 (23), 4250–4271.
Zheng, L.Y., Chi, Y.W., Dong, Y.Q., Lin, J.P., Wang, B.B., 2009. J. Am. Chem. Soc. 131 (13), 4564–4565.
Zhuravlev, A., Zacharia, A., Gucer, S., Chebotarev, A., Arabadji, M., Dobrynin, A., 2015. J. Food Compos. Anal. 38, 62–68.